



Co₃O₄ nanofiber as a high-performance electrocatalyst for oxygen evolution

Qingqing Wang¹ · Xianghui Wang¹ · Chongtai Wang¹ · Xiaobao Li¹ · Xiaohong Gao² · Chenghang You²

Received: 27 February 2022 / Revised: 30 May 2022 / Accepted: 11 June 2022 / Published online: 27 June 2022
© The Author(s), under exclusive licence to Springer-Verlag GmbH Germany, part of Springer Nature 2022

Abstract

Developing highly active and low-cost catalysts towards oxygen evolution reaction (OER) is of high importance for many advanced energy technologies, e.g., rechargeable fuel cells, metal-air batteries, water and splitting. In this work, Co₃O₄ nanofibers are prepared through a facile pyrolyzing procedure by using cobalt complex nanofibers as the precursor. The catalyst exhibits high performance towards OER in 1 M KOH solution, with potentials of 1.53 and 1.59 V at 10 and 100 mA cm⁻², respectively. When used as the air electrode catalyst combining with Pt/C catalyst, it can give the zinc-air battery a high charging performance, as well as an outstanding cyclic charging-discharging stability.

Keywords Co₃O₄ nanofiber · Oxygen evolution reaction · High-performance · Electrocatalysts · Rechargeable zinc-air battery

Introduction

Oxygen evolution reaction (OER) is a key process in many advanced energy technologies, e.g., rechargeable fuel cells [1], metal-air batteries [2–6], and water splitting [7–10]. Due to its sluggish kinetic procedures, highly active catalysts are required. Although noble metals like Ir and Ru, including their oxides, are the state-of-art catalysts for OER [11–14], their scarcity and high cost have seriously hampered their commercial applications. Thus, developing highly active and low-cost OER catalysts becomes rather important for the large-scale applications of these advanced energy technologies.

Co₃O₄ has a typical spinel structure, in which the tetrahedral and octahedral positions are occupied by Co²⁺ and Co³⁺, respectively. The coexistence of Co²⁺ and Co³⁺ make Co₃O₄ more conductive and beneficial to the reversible adsorption of molecular oxygen. Thus, Co₃O₄ can exhibit relatively high OER performance [7, 15–17]. Unfortunately, up to now, Co₃O₄-based OER catalysts still fail to meet the practical demands of those advanced energy technologies.

Generally, catalysts' performance can be enhanced by simply reducing their sizes to nanoscale thanks to the enlarged surface areas, the increased exposed active sites, and the improved contact between the catalyst and the support. However, as is well known, nano particles will easily agglomerate due to their high surface energy, which will eventually lead to the dramatic degradation in their catalytic performance. Nanofiberous structures can be attractive due to their inherent anisotropy, high flexibility, and high electrical conductivity. Compared with nano particles, nanofibers can avoid aggregation and maintain high surface areas effectively during the catalyzing procedures [18–20].

Inspired by these factors, nanofiberous Co₃O₄ will be charming since it combines the advantages of fibrous structures and Co₃O₄. In this work, we fabricated a nanofiberous Co₃O₄ catalyst through a facile pyrolyzing procedure by using a cobalt complex as the precursor. The catalyst exhibits high performance towards OER in 1 M KOH solution. The OER potentials can be as low as 1.53 and 1.59 V at 10

✉ Chongtai Wang
oehy2014@163.com

✉ Xiaobao Li
lixiaobao0797@163.com

✉ Chenghang You
youchh@163.com

¹ The Key Laboratory of Electrochemical Energy Storage and Energy Conversion of Hainan Province, School of Chemistry and Chemical Engineering, Hainan Normal University, Haikou 571158, China

² State Key Laboratory of Marine Resource Utilization in South China Sea, Hainan University, Haikou 570228, China

and 100 mA cm^{-2} , respectively. When used as the air electrode catalyst combining with Pt/C catalyst, it can deliver a zinc-air battery a high charging performance and an outstanding cyclic charging-discharging stability.

Experimental

Preparation of catalysts

The cobalt complex is firstly prepared through a procedure reported in our previous work [21]. Briefly, 7.0 mL CoCl_2 solution (0.15 M) and 3 mmol nitrilotriacetic acid are firstly added to 7.0 mL isopropanol (Fig. 1). After stirring for 10 min, the obtained mixture is transferred into an autoclave, which is then sealed and heated at $180 \text{ }^\circ\text{C}$ for 24 h. After cooling down naturally, the suspension is filtrated, rinsed with deionized water, and dried at $80 \text{ }^\circ\text{C}$ in a vacuum. The obtained pink powder is named as “NTACo.”

The Co_3O_4 nanofibers are prepared by pyrolyzing the precursor “NTACo” in air for 3 h under different temperatures, with a heating rate of $2 \text{ }^\circ\text{C min}^{-1}$. The obtained final catalysts are named as NTACo-400, NTACo-450, and NTACo-500, respectively, where the numbers stand for the temperatures applied.

Preparation of working electrodes

Five milligram catalyst is homogeneously dispersed in 1.00 mL Nafion ethanol solution (0.25 wt%) under ultrasound for about 30 min. Then, 20 μL of the obtained suspension is coated onto a glassy carbon electrode (GCE, Φ 5 mm) and dried naturally.

Preparation of air electrode

For catalyst layer fabrication, the slurry is firstly prepared by completely mixing NTACo-450 (5.0 mg) and Pt/C catalyst (5.0 mg) in Nafion ethanol solution (0.25 wt%, 2 mL) under ultrasonic. Subsequently, 100 μL of the obtained slurry is painted onto the gas diffusion layer (GDL, SIGRACET) and dried under an infrared lamp. The catalyst loading is calculated to be 0.5 mg cm^{-2} . For comparisons, mixed catalyst of Pt/C and Ir/C (with mass ratio of 1:1) is also used to fabricate a reference air electrode through the same procedures.

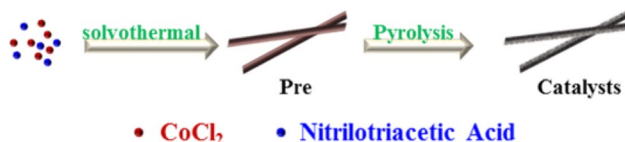


Fig. 1 Schematic illustration of catalysts' preparation

Characterization

The scanning electron microscopy (SEM) images are obtained on a JSM-7100F field emission scanning electron microscope (JEOL, Japan), with an acceleration voltage of 5 kV. The transmission electron microscopy (TEM) is operated on a JEM-2100 transmission electron microscope (JEOL, Japan) with an acceleration voltage of 200 kV. The X-ray photoelectron spectroscopy (XPS) is conducted on an ESCALAB 250 X-ray photoelectron spectrometer (Thermo-VG Scientific, USA). The X-ray diffraction (XRD) is conducted on a TD-3500 powder diffractometer (Tongda, China) at a scan rate of 5°min^{-1} .

Electrochemical measurements

Catalysts' electrochemical performance are evaluated by using a three-electrode glass cell on an Interface 1010B electrochemical workstation (Gamry, USA), coupled with a rotating disk electrode (RDE) system (RDE710, Gamry, USA). During the test, an Hg/HgO/NaOH (1 M) and Pt wire are used as the reference and counter electrodes, respectively. The GCE's geometric area is calculated to be 0.1964 cm^2 . And all the potentials initially measured are converted to the ones versus the reversible hydrogen electrode (RHE) by adding 0.92 V.

The linear sweep voltammetry (LSV) measurements are conducted at a scan rate of 5 mV s^{-1} . The *i*-*t* curves are recorded at 0.72 V (vs. RHE).

Battery tests

A home-made ZAB device is fabricated for the tests. A 6 M KOH solution containing 0.2 M zinc acetate is used as the electrolyte, and a zinc plate is used as the anode. The cyclic charging-discharging tests are conducted by using galvanostatic technology on a BTS-3000 battery testing system (Newware, China) under the current density of 5 mA cm^{-2} , with a duration time of 20 min for each cycle (10 min for discharging and another 10 min for charging).

Results and discussions

Figure 2 shows the SEM images of the precursor NTACo and the catalysts obtained at different temperatures. It can be seen that NTACo and the obtained catalysts all present nanofiberous morphologies, indicating that this nanofiberous morphology can be well preserved during the heat treatments. At the same time, we also noticed that the three catalysts obtained after heat treatment are composed by

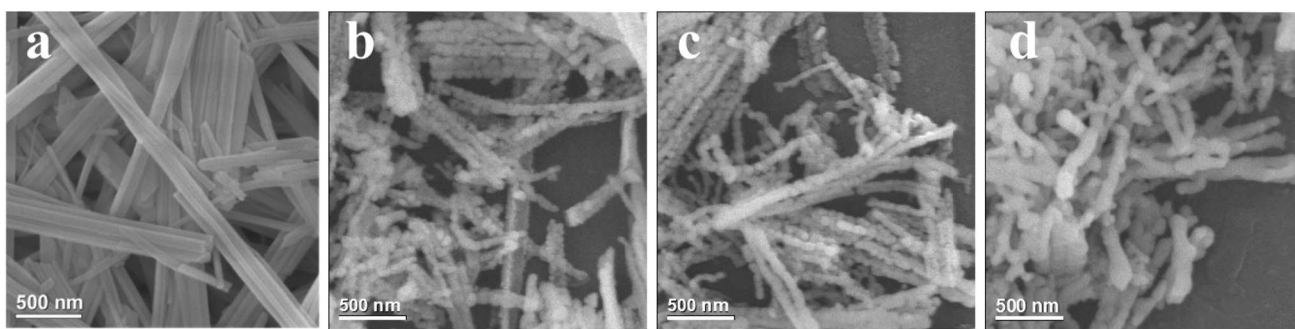


Fig. 2 SEM images: **a** NTACo; **b** NTACo-400; **c** NTACo-450; **d** NTACo-500

numerous nanoparticles, and the nanoparticles in NTACo-500 are significantly larger than those in NTACo-400 and NTACo-450, which can be further confirmed by their TEM images (Fig. 3a–c). Obviously, higher temperature promotes the agglomeration and aging of these nanoparticles.

From the high-resolution TEM (HRTEM) results, one can find that the lattice fringe spacing of the particle in NTACo-450 is about 0.29 nm (Fig. 3d), which can be assigned to the (220) crystal planes of Co_3O_4 , indicating that these particles are Co_3O_4 . Figure 3e–h is the EDS mapping results of NTACo-450. It can be found that Co, O, C, and N are homogeneously distributed in NTACo-450.

From the XRD patterns of the three catalysts (Fig. 4), the diffraction peaks around 19.0, 31.2, 36.8, 38.5, 44.8, 55.6, 59.3, and 65.2 degrees can be observed, which are

corresponding to the (111), (220), (311), (222), (400), (331), (422), and (440) facets of Co_3O_4 , indicating the existence of Co_3O_4 in the three catalysts. And these results are consistent with the HRTEM results.

Figure 5a shows the XPS spectra of NTACo and the catalysts obtained after the heat treatments. No obvious N1s peaks can be observed in the obtained catalysts. Given the surface atomic compositions (Fig. 5b), it can be found that the N contents decrease drastically from 8.3 to 0.6, 0.5, and 0.4 at% for NTACo-400, NTACo-450, and NTACo-500, respectively, suggesting that most of the nitrogenous organic components have been destroyed during the pyrolyzing process.

From the high-resolution Co2p spectrum of NTACo (Fig. 6a), two groups of peaks can be found between

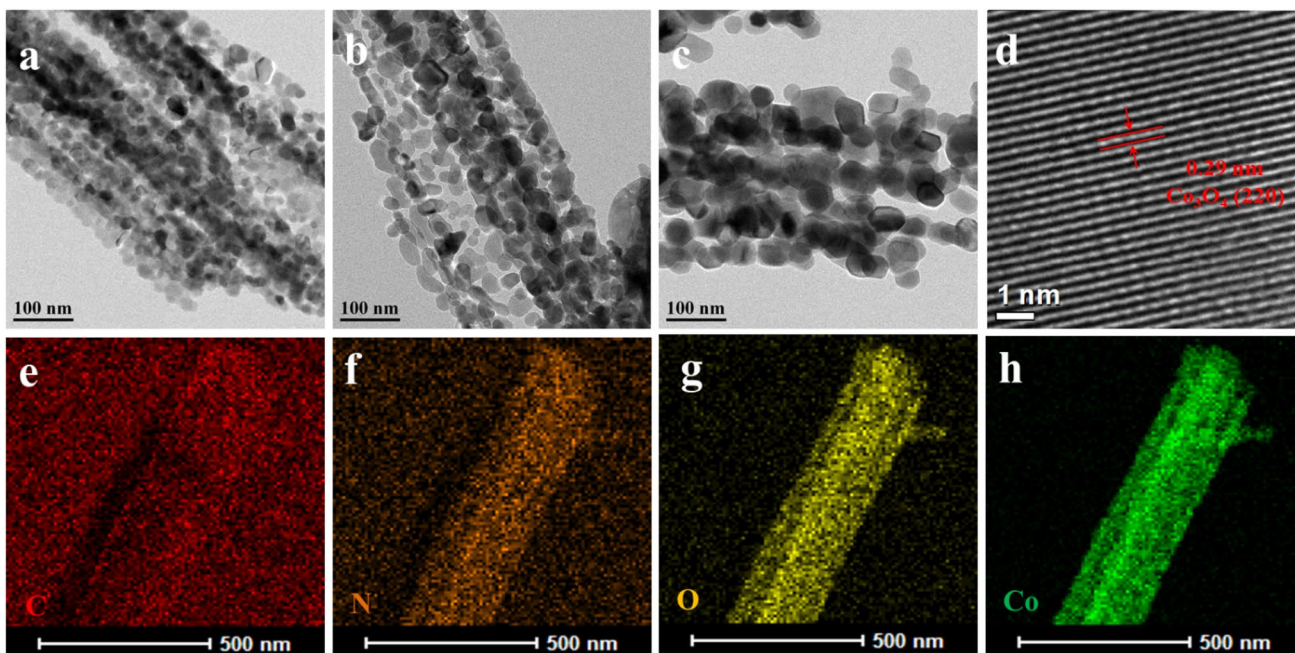


Fig. 3 **a** TEM image of NTACo-400; **b** TEM image of NTACo-450; **c** TEM image of NTACo-500; **d** HRTEM image of NTACo-450; **e–h** EDS mapping images of C, N, O, and Co in NTACo-450

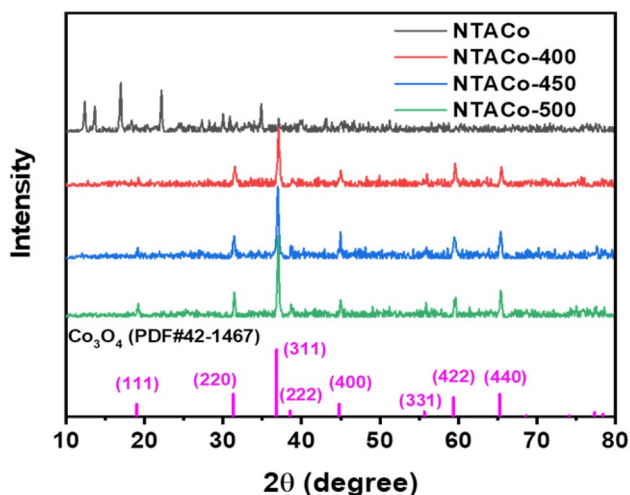


Fig. 4 XRD patterns for NTACo and catalysts obtained at various temperatures

810–793 and 793–775 eV, corresponding to the $\text{Co}2p_{1/2}$ and $\text{Co}2p_{3/2}$, respectively. The fitting results showed that the $\text{Co}2p_{3/2}$ of NTACo can be deconvoluted into three peaks around 780.0, 783.4, and 787.2 eV, which can be assigned to the Co(II)-OCO (carboxyl group), Co(II)-N , and Co satellite peaks, respectively [22]. Similarly, the $\text{Co}2p_{1/2}$ peak can be also deconvoluted.

Figure 6b–d shows the $\text{Co}2p$ spectra of the three catalysts. It can be seen that the $\text{Co}2p$ spectra of the three catalysts all show two groups of peaks around 795 and 780 eV, which are corresponding to the $\text{Co}2p_{1/2}$ and $\text{Co}2p_{3/2}$, respectively. The fitting results show that the $\text{Co}2p$ spectra can be separated into two peaks corresponding to Co^{3+} (around 794.6 and 779.5 eV) and Co^{2+} (around 796.5 and 781.2 eV), respectively, indicating that Co^{3+} and Co^{2+} coexist in the three catalysts. Considering the atomic compositions (Fig. 6e), it can be found that the NTACo-450 has the highest Co^{3+} content of 46.1 at% among the three catalysts.

Figure 7a shows the LSV curves of the different catalysts. It can be found that all the three catalysts exhibit

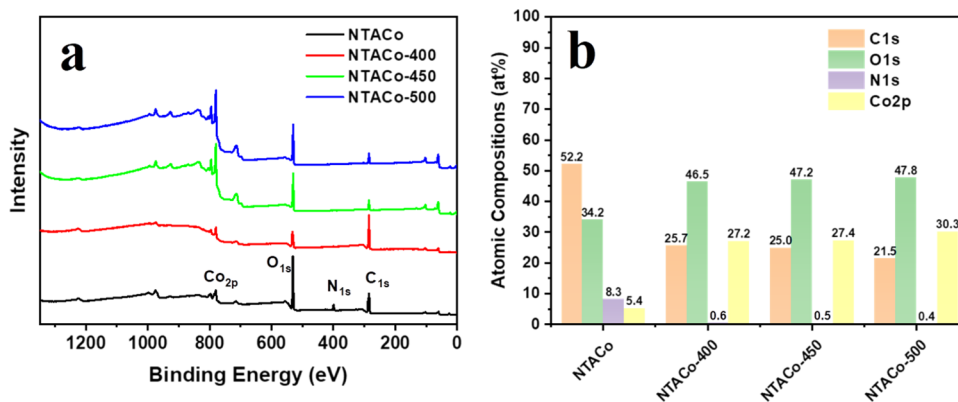
high OER catalytic performance, and outperform the Ir/C catalyst, especially at high current density. Among the three catalysts, NTACo-450 has the lowest potentials of 1.53 and 1.59 V (vs. RHE) at 10 and 100 mA cm^{-2} , respectively, indicating that NTACo-450 is the most active among the three catalysts. Figure 7c shows the Tafel slopes. It can be seen that the Tafel slopes of the three catalysts are 64.1, 59.1, and 63.2 mV dec^{-1} , respectively. Obviously, NTACo-450 has the lowest Tafel slope value, indicating that it has the lowest overpotential in catalyzing OER, which further confirms its highest OER performance among the three.

For Co_3O_4 , both Co^{2+} and Co^{3+} are regarded as the active sites for OER. However, some recent studies [23] discovered that Co^{3+} is actually much more active than Co^{2+} . Combining with the XPS results, NTACo-450 has the highest Co^{3+} content, which should be the proper reason for its highest OER performance among the obtained catalysts.

To evaluate the catalysts' performance in actual batteries, ZABs are fabricated. As illustrated in Fig. 7e, the ZAB using Pt/C + NTACo-450 composite catalyst exhibits a high current density of 203.4 mA cm^{-2} at 0.7 V, obviously higher than that of the ZAB using Pt/C + Ir/C catalyst (186.4 mA cm^{-2}). Regarding the charging performance, the ZAB using NTACo-450 can exhibit a rather high current density of 148.4 mA cm^{-2} at 2.2 V, which is much higher than that of ZAB using Ir/C catalyst (78.2 mA cm^{-2}), suggesting its better charging performances.

Figure 7f demonstrates the cyclic charging-discharging curves of the fabricated ZABs. During the first 100 cycles, the ZABs using Ir/C as the OER catalyst shows a rapid degradation in charging performance, whereas no significant performance decay was found for the one using NTACo-450. After 600 cycles, the ZABs using Pt/C and NTACo can maintain most of its initial performance, suggesting that it has a superior stability to that based on Pt/C and Ir/C.

Fig. 5 **a** XPS spectra for NTACo and obtained catalysts; **b** surface atomic compositions of NTACo and obtained catalysts from the XPS results



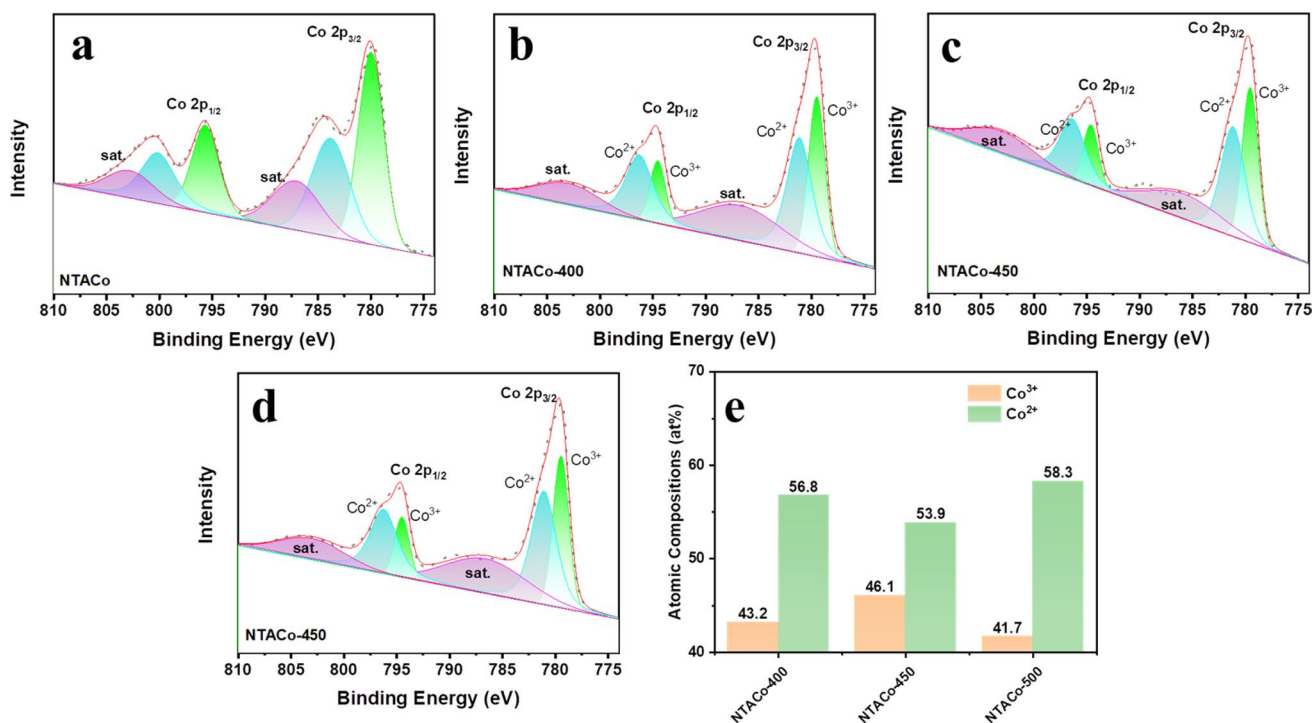


Fig. 6 High-resolution Co 2p XPS spectra: **a** NTACo; **b** NTACo-400; **c** NTACo-450; **d** NTACo-500; **e** atomic composition of Co2p in various catalysts

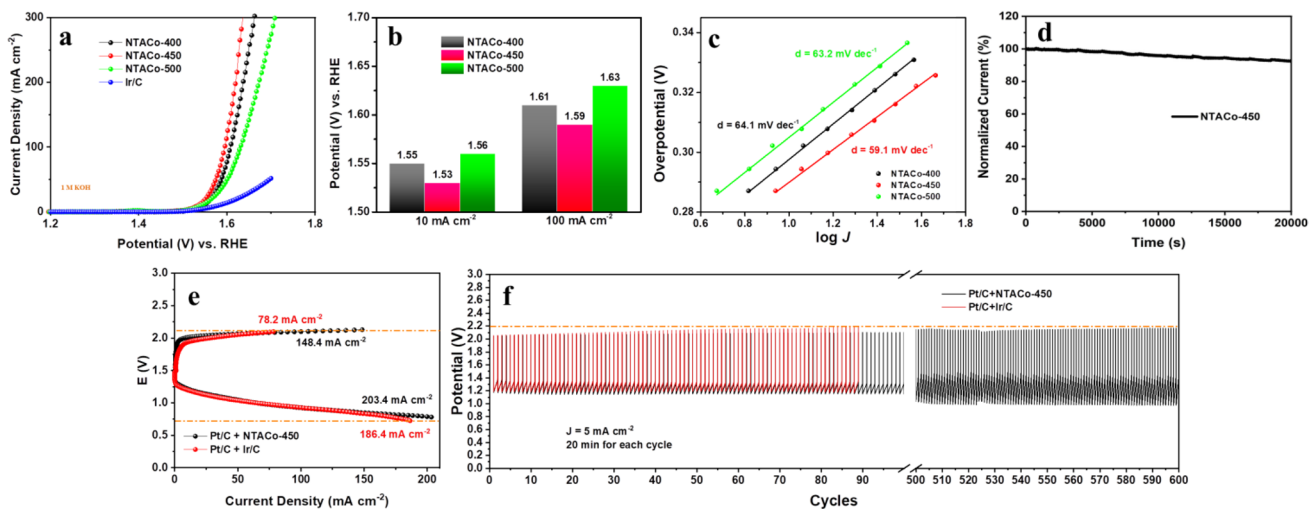


Fig. 7 **a** LSV curves in 1 M KOH solution of obtained catalysts; **b** OER potentials at 10 and 100 mA cm⁻², respectively; **c** Tafel curves derived from the LSV curves; **d** i-t curve of NTACo-450 after

a 20,000-s test at 0.72 V (vs. RHE); **e** charging-discharging curves of ZABs using different air electrode catalysts; **f** cyclic charging-discharging curves of ZABs using different catalysts

Conclusion

In summary, a Co₃O₄ nanofiber is prepared through a facile pyrolyzing procedure by using a cobalt complex prepared from cobalt chloride and nitrilotriacetic acid as the precursor. The catalyst

exhibits high performance towards OER in 1 M KOH solution, with potentials of 1.53 and 1.59 V at the current densities of 10 and 100 mA cm⁻², respectively. Specially, when used as the air electrode catalyst combining with Pt/C catalyst, it can deliver a zinc-air battery an outstanding cyclic charging-discharging stability.

Funding This work was supported by the Natural Science Foundation of Hainan Province (project Nos. 221RC540, 219QN206); the National Natural Science Foundation of China (NSFC project nos. 52162027, 21606061, 21805104, 31360069, 21662012, 51663009); the Development Program for Innovative Research Team in Ministry of Education (grant No. IRT-16R19); the Research Project of Hainan Provincial Department of Education (Hnky2017-21); Hainan Provincial Graduate Innovation Research Project (Hyb2020-53, Hys2019-278); the science and technology planning project of Haikou (2016030); and the Research Fund Program of Key Laboratory of Fuel Cell Technology of Guangdong Province.

References

- Dresp S, Luo F, Schmack R, Kühl S, Glied M, Strasser P (2016) An efficient bifunctional two-component catalyst for oxygen reduction and oxygen evolution in reversible fuel cells, electrolyzers and rechargeable air electrodes. *Energy Environ Sci* 9(6):2020–2024
- Zhao C-X, Liu J-N, Yao N, Wang J, Ren D, Chen X, Li B-Q, Zhang Q (2021) Can aqueous zinc–air batteries work at sub-zero temperatures? *Angew Chem Int Ed* 60(28):15281–15285
- Zhang Q, Guan J (2021) Applications of Atomically dispersed oxygen reduction catalysts in fuel cells and zinc-air batteries. *Energy Environ Mater* 4(3):307–335
- Wu W, Liu Y, Liu D, Chen W, Song Z, Wang X, Zheng Y, Lu N, Wang C, Mao J, Li Y (2021) Single copper sites dispersed on hierarchically porous carbon for improving oxygen reduction reaction towards zinc-air battery. *Nano Res* 14(4):998–1003
- Sun H, Wang M, Zhang S, Liu S, Shen X, Qian T, Niu X, Xiong J, Yan C (2020) Boosting oxygen dissociation over bimetal sites to facilitate oxygen reduction activity of zinc-air battery. *Adv Func Mater* 31(4):2006533
- Han J, Bao H, Wang J-Q, Zheng L, Sun S, Wang ZL, Sun C (2021) 3D N-doped ordered mesoporous carbon supported single-atom Fe-N-C catalysts with superior performance for oxygen reduction reaction and zinc-air battery. *Appl Catal B* 280:119411
- Yu M, Budiyanoto E, Tuysuz H (2022) Principles of water electrolysis and recent progress in cobalt-, nickel-, and iron-based oxides for the oxygen evolution reaction. *Angew Chem Int Ed Engl* 61(1):e202103824
- Liu S, Lin Z, Wan R, Liu Y, Liu Z, Zhang S, Zhang X, Tang Z, Lu X, Tian Y (2021) Cobalt phosphide supported by two-dimensional molybdenum carbide (MXene) for the hydrogen evolution reaction, oxygen evolution reaction, and overall water splitting. *J Mater Chem A* 9(37):21259–21269
- Zhuang L, Jia Y, Liu H, Li Z, Li M, Zhang L, Wang X, Yang D, Zhu Z, Yao X (2020) Sulfur-modified oxygen vacancies in iron-cobalt oxide nanosheets: enabling extremely high activity of the oxygen evolution reaction to achieve the industrial water splitting benchmark. *Angew Chem Int Ed* 59(34):14664–14670
- Jin R, Huang J, Chen G, Chen W, Ouyang B, Chen D, Kan E, Zhu H, Li C, Yang D, Ostrikov K (2020) Water-sprouted, plasma-enhanced Ni-Co phospho-nitride nanosheets boost electrocatalytic hydrogen and oxygen evolution. *Chem Eng J* 402:126257
- You C, Gao X, Wang Q, Li X, Tan S, Xu P, Cai D, Weng Y, Wang C, Tian X, Liao S (2019) Rechargeable zinc–air battery with ultra-high power density based on uniform N Co codoped carbon nanospheres. *ACS Appl Mater Interfaces* 11(47):44153–44160
- Zhu Y, Yue K, Xia C, Zaman S, Yang H, Wang X, Yan Y, Xia BY (2021) Recent advances on MOF derivatives for non-noble metal oxygen electrocatalysts in zinc-air batteries. *Nanomicro Lett* 13(1):137
- Wu M, Zhang G, Du L, Yang D, Yang H, Sun S (2021) Defect electrocatalysts and alkaline electrolyte membranes in solid-state zinc-air batteries: recent advances, challenges, and future perspectives. *Small Methods* 5(1):e2000868
- Wang SY, Chen SM, Ma LT, Zapfen JA (2021) Recent progress in cobalt-based carbon materials as oxygen electrocatalysts for zinc-air battery applications. *Mater Today Energy* 20:100659
- Quast T, Varhade S, Saddeler S, Chen Y-T, Andronesco C, Schulz S, Schuhmann W (2021) Single particle nanoelectrochemistry reveals the catalytic oxygen evolution reaction activity of Co3O4 nanocubes. *Angew Chem Int Ed* 60(43):23444–23450
- Hu Z, Hao L, Quan F, Guo R (2022) Recent developments of Co3O4-based materials as catalysts for the oxygen evolution reaction. *Catal Sci Technol* 12(2):436–461
- Lu Y, Fan D, Chen Z, Xiao W, Cao C, Yang X (2020) Anchoring Co3O4 nanoparticles on MXene for efficient electrocatalytic oxygen evolution. *Sci Bull* 65(6):460–466
- Aljabour A (2020) Long-lasting electrospun Co3O4 nanofibers for electrocatalytic oxygen evolution reaction. *Chemistry Select* 5(25):7482–7487
- Wang Z, Liu H, Ge R, Ren X, Ren J, Yang D, Zhang L, Sun X (2018) Phosphorus-doped Co3O4 nanowire array: a highly efficient bifunctional electrocatalyst for overall water splitting. *ACS Catal* 8(3):2236–2241
- Xu Q-Z, Xu Q-Z, Su Y-Z, Wu H, Cheng H, Hui Y-P, Li N, Liu Z-Q (2014) Effect of morphology of Co3O4 for oxygen evolution reaction in alkaline water electrolysis. *Curr Nanosci* 11(1):107
- Wang Q, Gao X, Li X, You C, Wang C, Liao S (2021) Metallic cobalt encapsulated in N-doped carbon nanowires: a highly active bifunctional catalyst for oxygen reduction and evolution. *Ionics* 27(8):3501–3509
- Li C, Yin X, Chen L, Li Q, Wang T (2010) Synthesis of cobalt ion-based coordination polymer nanowires and their conversion into porous Co3O4 nanowires with good lithium storage properties. *Chem Eur J* 16(17):5215–5221
- Liu Z, Wang G, Zhu X, Wang Y, Zou Y, Zang S, Wang S (2020) Optimal geometrical configuration of cobalt cations in spinel oxides to promote oxygen evolution reaction. *Angew Chem* 132(12):4766–4772

Publisher's note Springer Nature remains neutral with regard to jurisdictional claims in published maps and institutional affiliations.